IEEE Access
Multidisciplinary | Rapid Review | Open Access Journal

IEEE ENGINEERING IN MEDICINE AND BIOLOGY SOCIETY SECTION

Received June 11, 2021, accepted July 12, 2021, date of publication July 19, 2021, date of current version July 27, 2021.

Digital Object Identifier 10.1109/ACCESS.2021.3098039

Electrocardiographic Machine Learning to Predict Mitral Valve Prolapse in Young Adults

GEN-MIN LIN[1,2], (Member, IEEE), AND HUAN-CHANG ZENG[3]

[1]Department of Medicine, Hualien Armed Forces General Hospital, Hualien 97144, Taiwan
[2]Department of Medicine, Tri-Service General Hospital, National Defense Medical Center, Taipei 11490, Taiwan
[3]GENEus Medical Technology Company Ltd., Taipei 11069, Taiwan

Corresponding author: Gen-Min Lin (farmer507@yahoo.com.tw)

This work was supported in part by the Medical Affairs Bureau, Ministry of National Defense, Taiwan, under Grant MND-MAB-110-148, and in part by Hualien Armed Forces General Hospital, Taiwan, under Grant HAFGH-D-110008.

This work involved human subjects or animals in its research. Approval of all ethical and experimental procedures and protocols was granted by the Institutional Review Broad of the Mennonite Christian General Hospital, Hualien City, Taiwan, under Approval No. 16-05-008.

ABSTRACT Mitral valve prolapse (MVP), known as balloon mitral valve, accounts for 2-4% of cases in the general population and is associated with several cardiac sequelae. A few studies have shown suboptimal results using electrocardiographic (ECG) machine learning to identify MVP in middle- or old-aged individuals; however, no studies have focused on young adults. The aim of this study is to develop an ECG-based system through machine learning to predict MVP in young adults. In a large military population of 2,206 males, aged 17-43 years, support vector machine (SVM), logistic regression (LR) and multilayer perceptron (MLP) classifiers are used as machine learning techniques for 26 ECG features and additional 6 simple biological parameters to link the output of MVP compared with a traditional ECG criterion of a negative T-axis in inferior limb leads. In the parasternal long-axis view of echocardiography, MVP is defined as a displacement of the anterior or posterior leaflet of the mitral valve to the mid portions of the annular hinge point >2 mm. The values of the area under the receiver operating characteristic curve are 74.59%, 74.16% and 73.02% in the proposed SVM, LR and MLP classifiers, respectively, which are better than 38.13% in the traditional ECG criterion for MVP. Our machine learning system provides a novel tool for screening MVP among young male adults. The proposed method can be an adjuvant to the physical findings for early detection of MVP prior to a confirmation by echocardiography for young male adults.

INDEX TERMS Echocardiography, electrocardiography, machine learning, mitral valve prolapse, young adults.

I. INTRODUCTION

Mitral valve prolapse (MVP), known as balloon mitral valve, accounts for 2-4% of cases in the general population [1]–[5]. There are several types of MVP classified by the presence or absence of syndromic and familial inheritance [6]–[11]. Syndromic MVP commonly presents with connective tissue diseases, such as Marfan syndrome and Ehlers-Danlos syndrome [7]–[9]. Regarding familial nonsyndromic MVP, inheritance is possibly autosomal dominant and age- and sex-dependent [8]–[10]. Other types are classified as sporadic nonsyndromic MVP [10], [11]. A floppy mitral valve plays a pivotal role in the pathogenesis of MVP [12], [13] and can be easily assessed by echocardiography and physical examinations. A substantial proportion of young people with MVP have several somatic symptoms including chest pain, palpitation and intolerance to heavy exercise, possibly due to autonomic neural feedback and low stroke volume related to MVP [11]. Although the Framingham Heart Study reported that MVP was associated with a low incidence of complications in the general population [1], many case studies have revealed that those with MVP have a higher risk of bacterial endocarditis [14], [15], ischemic stroke [16], severe mitral regurgitation [2], [4], [17], and complicated ventricular arrhythmias [18], [19]. As early as 30 years of age or older, the presence of a mitral systolic click can be physically auscultated in 10-20% of patients with MVP [12], [13], depending on the severity of the MVP

The associate editor coordinating the review of this manuscript and approving it for publication was Behrouz Shabestari.

and the mitral regurgitation [13]. Early screening of MVP in young adults is crucial for confirmation by echocardiography, which may facilitate a decision making made by primary physicians in specific clinical situations, e.g., antibiotic prophylaxis during surgery to prevent the occurrence of bacterial endocarditis related to MVP [20].

A few studies have reported that most patients with MVP present T-wave inversions in inferior limb leads II, III and aVF as a typical feature in 12-lead surface electrocardiography (ECG), which may be a practical tool for screening for the presence of MVP in the general population [21], [22]. Machine learning methods are a kind of artificial intelligence for computational statistics and have been introduced widely in medicine to provide accurate and fast diagnosis for and in the prediction of various diseases [23]–[30]. A study by Tison *et al.* utilized the gradient boost machine (GBM) classifier for a number of ECG features to predict MVP in a large population of middle- and old-aged individuals [31], and the results revealed that the area under curve (AUC) of the receiver operating characteristic (ROC) curve was suboptimal, with an estimate of up to 77%. However, there have been no studies on young adults thus far.

In this paper, we aim to develop a clinically available 12-lead ECG-based system that utilizes a large sample size of military young males, taking age, anthropometric variables, hemodynamics and ECG features into account for machine learning to predict the presence of MVP as shown in Fig. 1. The rest of this paper is presented as follows. The materials are summarized in Section II. In Section III, the proposed algorithms regarding the ECG system in the detection of MVP are described in detail. Section IV presents the experimental results. Section V concludes this paper.

II. DATA COLLECTION AND FEATURES SELECTION

This study uses a population of 2,206 military males, aged 17-43 years from an ancillary study of cardiorespiratory fitness and hospitalization events in armed forces (CHIEF) performed in the Hualien Armed Forces General Hospital in Taiwan. Each study participant received a 12-lead ECG and a transthoracic echocardiography in an annual health examination revisit for military awards or a promotion of rank. This study protocol has been described in detail before [32]–[42]. The ECG data are processed and interpreted by the software products of CARDIOVIT MS-2015 (Schiller AG, Baar, Switzerland) and the CARDIOGRAPH TC70 (Philips, Amsterdam, Netherlands). The echocardiography is carried out via an IE33 machine (Philips, Amsterdam, Netherlands) by an experienced technician. The software for each ECG machine gives an analysis of the amplitudes, durations, and morphologies of the ECG waveforms. The analysis of ECG is established according to standard criteria for interpretation of the parameters, calculations of the electrical axis, and the relationship between leads. The algorithm produces precise and consistent ECG measurements that are used to generate interpretive statements. As the aim of this study is to develop a convenient ECG-based system for MVP, the most common 26 ECG parameters from commercially available software were thus adopted as the inputs for machine learning including heart rate, PR, QRS and QT intervals, P wave duration and P, QRS, and T-wave axes in Lead II, R wave voltages in both the limb and precordial leads and S wave voltages in the precordial leads. In addition to the 26 adopted ECG features mentioned above, 6 biological features including age, body height, body weight, waist size, systolic blood pressure and diastolic blood pressure, are also treated as the inputs in the proposed machine learning models. The comparison uses the T-wave axis in Lead II, the only ECG criterion for MVP based on previous study findings [21], [22]. MVP is diagnosed by echocardiography if a displacement of the anterior or posterior leaflet of mitral valve to the mid portions of the mitral annular hinge point >2 mm in the parasternal long-axis window, based on the latest suggestion from the American Society of Echocardiography [1], and is set as the output of the machine learning models. The MVP characters to show echo features for the subjects are described in Table 1. The baseline profiles of participants with MVP and those without MVP are expressed as the mean $\pm$ standard deviation and are compared by two-sample t-tests in Table 2. A value of $p < 0.05$ is considered significant. The CHIEF heart study was reviewed and approved by the Institutional Review Broad of the Mennonite Christian General Hospital (No. 16-05-008) in Hualien City, Taiwan.

TABLE 1. Characters of mitral valve prolapse.

	Subjects with Mitral Valve Prolapse (N =74)
Mitral leaflet involvement	
Anterior mitral leaflet	21 (28 %)
Posterior mitral leaflet	43 (58 %)
Bi-mitral leaflets	10 (14 %)
Mitral regurgitation degree	
Trivial or Mild	56 (76 %)
Moderate or Severe	6 (8 %)
None	12 (16%)

III. PROPOSED METHOD

This paper proposes to utilize three machine learning classifiers, namely, support vector machine (SVM), logistic regression (LR) and multilayer perceptron (MLP), for a total of 32 biological and ECG features training to predict MVP among young adults. The flowchart of the proposed method is illustrated in Fig. 2.

A. DATA NORMALIZATION

To overcome the issue of various ranges of the input features, the original data of the 32 adopted biological and ECG features are individually normalized by a linear transformation into a value between 0 and 1, also known as the min-max scaling [43]. The equation of the min-max normalization is calculated using Eq. (1), where each of the actual data a

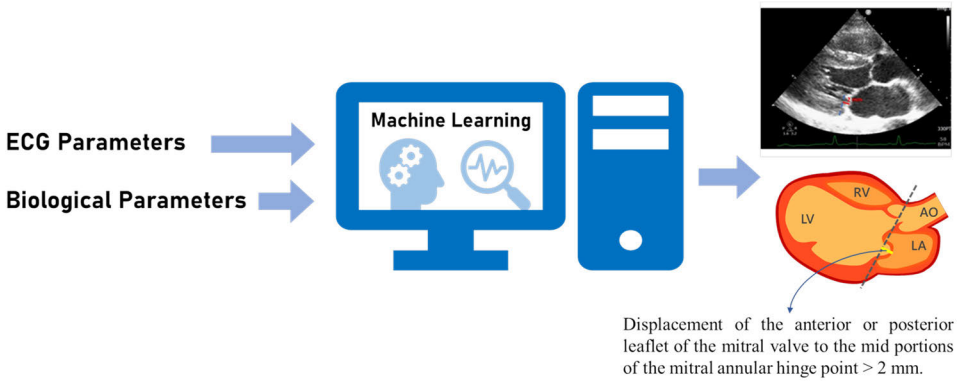

FIGURE 1. Schematic diagram of proposed MVP prediction system.

TABLE 2. Characteristics of study participants.

Features	Total N=2206	Non-MVP N=2132	MVP N=74	p-value
Age (years)	27.99±6.16	28.04±6.17	26.53±5.98	0.0376
Height (cm)	172.16±5.77	172.15±5.79	172.33±5.21	0.7913
Weight (kg)	74.00±12.30	74.11±12.32	70.89±11.35	0.0267
Waist (cm)	83.80±9.89	83.88±9.87	81.51±10.09	0.0422
SBP (mmHg)	119.65±13.43	119.74±13.34	117.16±15.64	0.1663
DBP (mmHg)	71.06±10.52	71.05±10.49	71.18±11.52	0.9258
Heart rate (bpm)	66.50±10.85	66.53±10.84	65.72±11.12	0.5264
P-II (ms)	106.67±14.70	106.78±14.72	103.49±13.99	0.0589
PR-II (ms)	157.80±20.14	157.81±20.13	157.34±20.35	0.8426
QRS-II (ms)	97.69±10.81	97.64±10.83	99.05±10.12	0.2692
QT-II (ms)	372.67±27.77	372.65±27.75	373.00±28.32	0.9159
P axis-II (degree)	44.21±24.64	44.25±24.50	42.98±28.52	0.6612
QRS axis-II (degree)	61.63±32.00	61.42±32.12	67.68±28.07	0.0984
T axis-II (degree)	33.82±20.52	33.60±20.56	40.30±18.33	0.0058
R-I (mm)	6.07±3.04	6.10±3.03	5.13±3.30	0.0068
R-II (mm)	12.43±4.93	12.47±4.94	11.37±4.55	0.0600
R-III (mm)	7.79±5.66	7.80±5.68	7.67±4.96	0.8471
R-aVR (mm)	1.32±1.81	1.30±1.78	1.97±2.45	0.0223
R-aVL (mm)	3.04±2.52	3.03±2.53	3.33±2.45	0.3100
R-aVF (mm)	9.90±5.24	9.91±5.26	9.47±4.79	0.4793
R-V1 (mm)	3.40±2.13	3.42±2.14	2.84±1.71	0.0059
S-V1 (mm)	9.88±5.05	9.86±5.05	10.21±5.08	0.5623
R-V2 (mm)	8.58±4.07	8.63±4.08	7.18±3.63	0.0026
S-V2 (mm)	15.40±6.63	15.36±6.62	16.60±6.68	0.1131
R-V3 (mm)	12.89±5.68	12.95±5.70	11.17±4.88	0.0081
S-V3 (mm)	8.51±5.16	8.48±5.14	9.55±5.89	0.0783
R-V4 (mm)	19.06±6.66	19.10±6.64	17.65±7.01	0.0639
S-V4 (mm)	5.47±4.02	5.46±4.00	5.90±4.60	0.3517
R-V5 (mm)	19.78±5.81	19.85±5.75	17.70±7.16	0.0126
S-V5 (mm)	3.49±2.92	3.48±2.93	3.66±2.81	0.6085
R-V6 (mm)	16.77±4.94	16.85±4.89	14.61±5.95	0.0020
S-V6 (mm)	2.12±2.01	2.13±2.02	2.07±1.52	0.7455

of the feature f is mapped to a normalized value, with the range between 0 and 1 for the subsequent process of machine learning:

$$Normalized\ (a) = a' = \frac{a - \min(f)}{\max(f) - \min(f)}, \qquad (1)$$

where a and a' represent the original and normalized data of feature f among the 32 input features, respectively, and $\min(f)$ and $\max(f)$ account for the minimum and maximum values of the input feature f, respectively.

B. CROSS-VALIDATION

The data of the 2,206 military male subjects are randomly divided into a training/validation set and a test set at a 3:1 ratio. The samples are divided into two parts: 75% for cross-validation (N = 1654 and MVP cases = 56) and 25% for testing (N = 552 and MVP cases = 18). The data numbers illustrated by 2-fold cross-validation are described in Table 3. The training/validation set is divided into two subgroups of equal size. Initially, one subgroup of the training/validation set is treated as the validation set, and another subgroup is

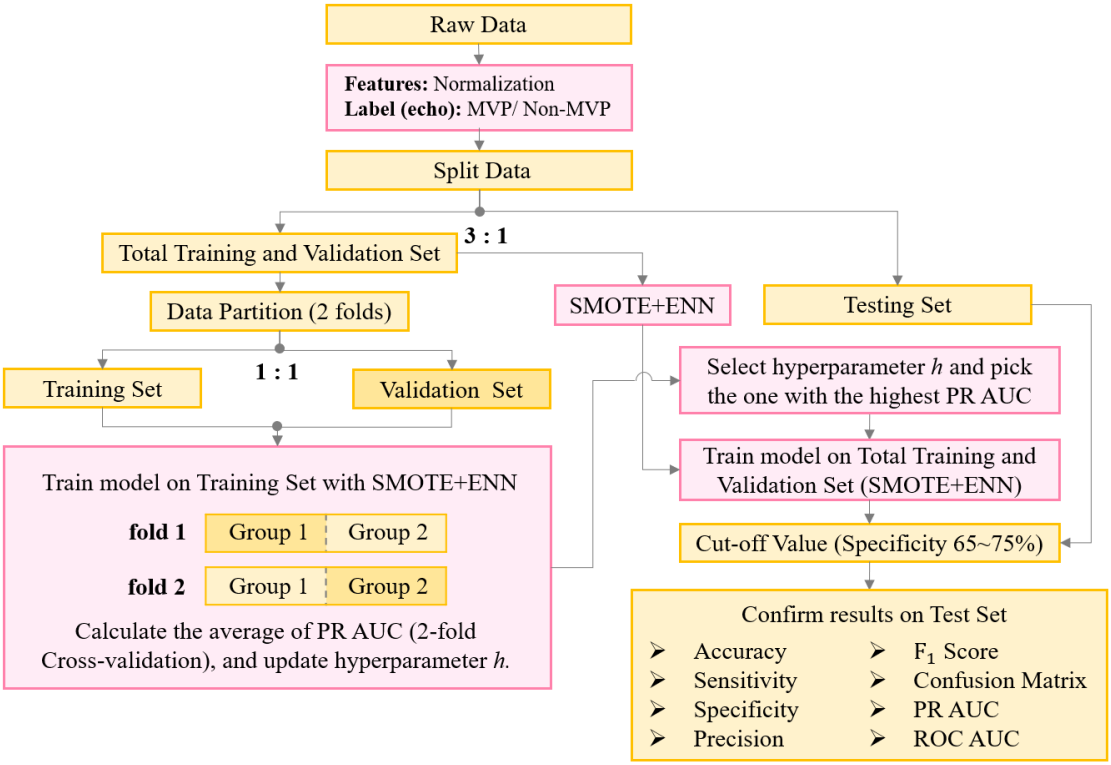

FIGURE 2. The flowchart of the proposed method.

TABLE 3. Data numbers in the dataset.

Fold	Data	Non-MVP	MVP	Total
1st	**Training Set**	803	24	827
	Pre-processed by SMOTE+ENN	803	517	1320
	Validation Set	795	32	827
2nd	**Training Set**	795	32	827
	Pre-processed by SMOTE+ENN	795	448	1243
	Validation Set	803	24	827
-	**Testing Set**	534	18	552

treated as the training set. Then, the process is repeated for an exchange of the roles of the two subgroups: one as the validation set and another as the training set. An average of the two AUCs of the precision recall (PR) curves from the two folds as a single performance is generated as the final result, from which a better generalization assessment of the performance for training can be obtained.

C. APPLICATION OF SMOTE AND ENN

The prevalence of MVP in military young adults is very low, estimated at 3.35%. Since there is an imbalance in sample size between non-MVP and MVP samples, we apply the synthetic minority oversampling technique (SMOTE) [44] and the edited nearest neighbor (ENN) technique [45] to artificially increase the MVP samples. The main idea of SMOTE is to create numerous new cases of minority class by randomly choosing a near neighbor of the minority class and interpolating as described in Eq. (2). First, for each sample of minority class X_p, its k nearest neighbors from other samples of minority class are taken. Subsequently, the minority class sample X_q among the k neighbors, is randomly selected. In the last step, X_{New} is generated as the synthetic sample by interpolating X_p and X_q:

$$X_{New} = X_p + rand\ (0,\ 1) * \left(X_q - X_p\right), \tag{2}$$

where $rand\ (0,\ 1)$ represents a generated random number between 0 and 1. From a geometric viewpoint, the process of utilizing SMOTE can be considered an interpolation between two MVP samples. The decision space for the MVP samples is thus magnified. The SMOTE method can balance the number of each category. However, it may cause the generated minority class samples and the original majority class samples to overlap so that they cannot be discriminated well. To solve this problem, we use the SMOTE+ENN method. In the training set, the ENN method is used to find t neighboring cases for the minority class cases (X_{New}) generated by SMOTE. If these t cases belong to the cases of the majority class, the cases of the minority class will be deleted. In this case, the SMOTE+ENN method can make the boundary of each class clearer and allows the proposed machine learning classifiers to have higher prediction performances on the unknown MVP samples. In this study, the SMOTE+ENN method as illustrated in Fig. 3, is utilized in the process of 2-fold cross-validation. The training data of the MVP group

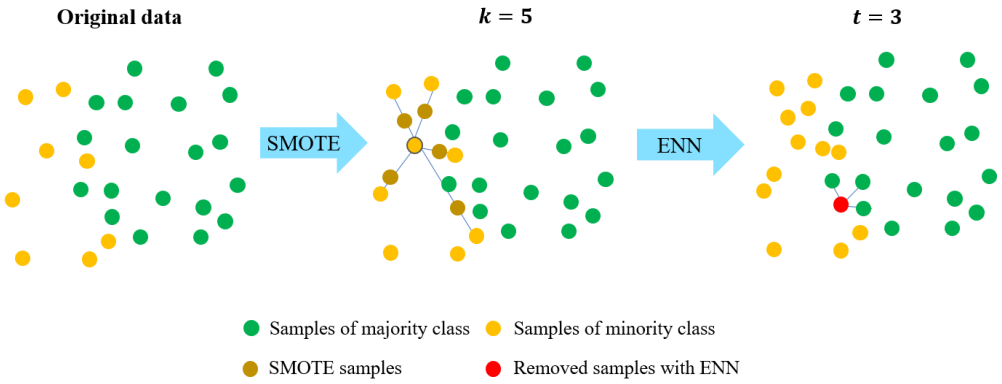

FIGURE 3. Illustration of SMOTE+ENN.

are preprocessed and increased by SMOTE+ENN to 517 and 448 for the two folds, respectively, as shown in Table 3.

D. MACHINE LEARNING MODEL

1) SUPPORT VECTOR MACHINE

A support vector machine (SVM) [46] with a linear kernel is used for our proposed approach. A data point is regarded as a 32-dimensional vector. The linear SVM separates such data points with the maximum-margin hyperplane which has the greatest distance to the nearest training points of non-MVP and MVP classes. The training data include the synthetic samples by SMOTE+ENN for MVP class. Considering that most of the data are nonlinearly separable data, we use soft-margin SVM as shown in Fig. 4. The regularization technique of adding the loss function by the squared hinge loss with hyperparameter is adopted to fit the training data. The $\ell 2$-norm is utilized in our SVM scheme. In the training process, the hyperparameter of soft-margin SVM decides the trade-off between the maximum margin and the correct classification of training data. The purpose of adjusting hyperparameter is also to reduce overfitting.

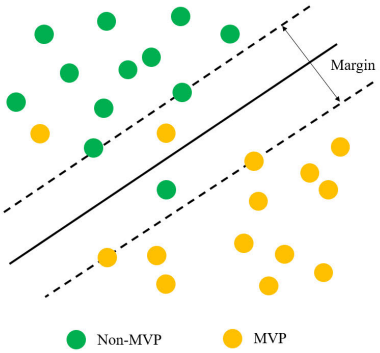

FIGURE 4. Soft-margin SVM.

2) LOGISTIC REGRESSION

Logistic regression (LR) [47], an extension of the linear regression model for the classification of two outcomes, is used in our method and illustrated in Fig. 5 and defined

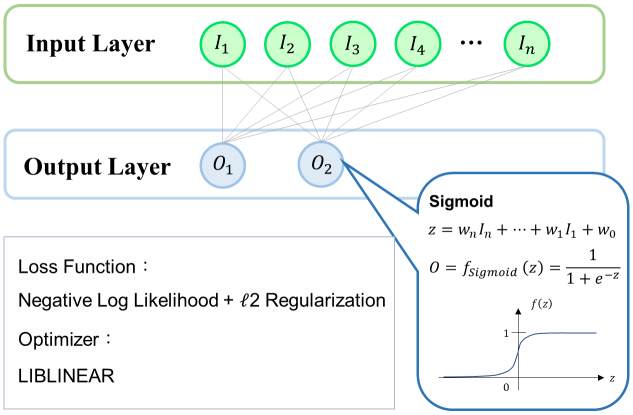

FIGURE 5. Logistic Regression.

in Eqs. (3) - (4):

$$z = w_n I_n + \cdots + w_1 I_1 + w_0, \tag{3}$$

$$O = f_{sigmoid}(z) = \frac{1}{1+e^{-z}}, \tag{4}$$

where $I_1 \sim I_n$ denote the input variables and n is 32 for the proposed scheme. The learned weights consist of $w_0 \sim w_n$. The output O returns a value of probability using the logistic sigmoid function.

The loss function is made of the loss term and the regularization term. The loss term of negative log-likelihood is for learning the weights $w_0 \sim w_n$. The regularization term $\ell 2$-norm to penalize large weights is implemented to prevent overfitting and improves the generalization capability. The choice of regularization hyperparameter is significant and optimized in our method.

3) MULTILAYER PERCEPTRON

A multilayer perceptron (MLP) [48] as illustrated in Fig. 6, which is composed of an input layer, some hidden layers and an output layer, is used in our method. In the fully connected MLP shown in Fig. 6, each node in one layer connects with every node in the next layer by a certain weight u_{in} as listed in Eqs. (5) - (6):

$$v_i = u_{in} I_n + \ldots + u_{i1} I_1 + u_{i0}, \tag{5}$$

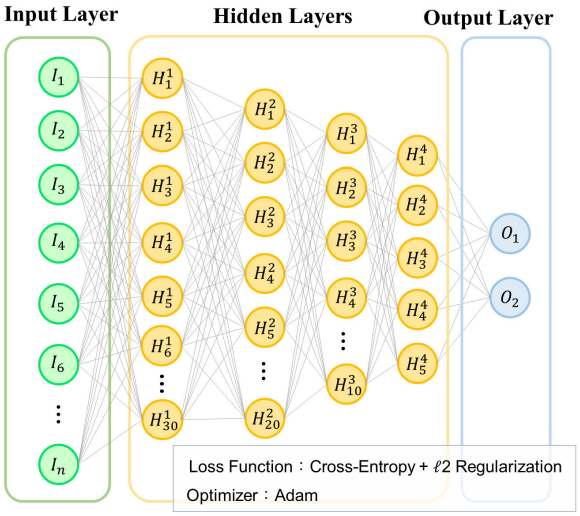

FIGURE 6. Multilayer perceptron.

$$H_i^k = f_{ReLU}\,(v_i), \tag{6}$$

where n indicates the number of input data ($I_1 \sim I_n$) or the number of neurons in the previous hidden layer and v denotes the weighted sum of the connections. For each node in hidden layers, the activation function rectified linear unit (ReLU) is carried out. H_i^k represents the output of the i-th node (neuron) of the k-th hidden layer. The logistic regression function determines the output layer O.

Forward propagation computes and stores the intermediate variables from the input layer through the hidden layers to the output layer. Back propagation calculates the gradients of the parameters by the Adam optimizer. Training involves adjusting the parameters to minimize the cross-entropy loss function. $\ell 2$-norm regularization is to prevent overfitting. The regularization hyperparameter is optimized in our proposed MLP classifier. The numbers of hidden layers, neurons and iterations are 4, 30, 20, 10, 5 and 1000, respectively.

IV. RESULTS AND DISCUSSION

This study utilizes scikit learn v0.20.2 software and Python programming language to implement the proposed methods [49]. In addition, the optimized hyperparameters are chosen by grid search, while the highest AUC of the PR curve averaged from 2-fold cross-validation is obtained. The hyperparameters of the three machine learning approaches are shown in Table 4. For example, the hyperparameter C for SVM is initialized to 0.0070. The training process with an increment of 0.0001 of C for the grid search is iterated until C reaches to 0.0150.

A. PERFORMANCE MEASUREMENT

The assessments of the performance [50] include the AUC of the ROC curve, the AUC of the PR curve, specificity, sensitivity (recall), accuracy, precision and the F_1 score.

Specificity, sensitivity (recall), accuracy and precision are defined and calculated by true positive (TP), true negative (TN), false positive (FP) and false negative (FN) results as revealed in Eqs. (7) - (10). The F_1 score, a harmonic average of the precision and recall, is denoted in Eq. (11).

$$Specificity = \frac{TN}{TN + FP}, \tag{7}$$

$$Sensitivity(Recall) = \frac{TP}{TP + FN}, \tag{8}$$

$$Accuracy = \frac{TP + TN}{TP + TN + FP + FN}, \tag{9}$$

$$Precision = \frac{TP}{TP + FP}, \tag{10}$$

$$F_1\ score = \frac{2 \times Precision \times Recall}{Precision + Recall}. \tag{11}$$

B. RESULTS

Table 5 displays the results of the testing set with the optimized hyperparameters. The prevalence of MVP in the young adults in the testing set is estimated to be 3.26%, as shown in Table 3. For the SVM, LR and MLP, the specificities are 69.85%, 72.10% and 70.04%, respectively; the sensitivities are 72.22% for all; the accuracies are 69.93%, 72.10%, and 70.11%, respectively; the precisions are 7.47%, 8.02% and 7.51%, respectively; and the F_1 scores are 13.54%, 14.44% and 13.61%, respectively. With regard to the traditional ECG criterion of a negative T-axis in inferior limb lead II for MVP, the specificity, sensitivity, accuracy, precision and F_1 score are 4.87%, 94.44%, 7.79%, 3.24% and 6.26%, respectively. The AUCs of the ROC and PR curves are compared in Fig. 7. The AUCs of the ROC curves are 74.59%, 74.16% and 73.02% for SVM, LR and MLP methods, respectively, which are much greater than 38.13% for the negative T-axis in inferior limb lead II. Similarly, the AUCs of the PR curves are 7.90%, 9.16% and 9.00% for the SVM, LR and MLP, respectively which are better than 2.59% for the negative T-axis in inferior limb lead II.

C. DISCUSSION

To the best of our knowledge, only one study by Tison *et al.* [31] has utilized the GBM machine learning classifier for ECG features training to predict MVP in middle- and old-aged individuals whose average age is 61 years. In [31], 1576 ECG studies from 356 patients with MVP were compared with 4864 ECG control studies from those without MVP, and the AUC of the ROC curve was approximately 77%. Our study utilizes different machine learning classifiers including SVM, LR and MLP for both biological and ECG features training to identify MVP in young adult males, yielding similar results in which the AUCs of the ROC curves are approximately 73-75%. In addition, this study discovers that although the presence of a negative axis of T-wave in inferior limb leads is a typical ECG feature and is prevalent (>94%) in individuals with MVP, the performance of MVP prediction is extremely low and assures that using the ECG criterion for the detection of MVP is clinically impractical.

TABLE 4. Hyperparameter optimization.

Model	Hyperparameter	Beginning value	Ending value	Interval	Optimal value
Support Vector Machine	Regularization	0.0070	0.0150	0.0001	0.0080
Logistic Regression	Regularization	0.0001	0.0100	0.0001	0.0010
Multilayer Perceptron	Regularization	0.001	0.100	0.001	0.010
	Number of Hidden Layers	1	5	1	4
	Number of Neurons	-	-	-	30, 20, 10, 5
	Number of Iterations	-	-	-	1000

The hyperparameters that are not described in this table are set to the default values used in the Scikit-learn library.

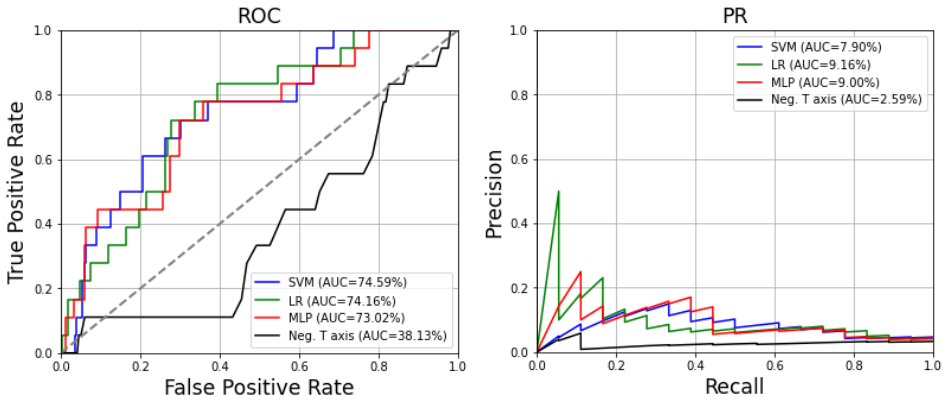

FIGURE 7. Receiver operating characteristic curves and precision recall curves.

TABLE 5. Performance comparison of proposed method and previous work.

	Specificity	Sensitivity	Accuracy	Precision	F_1 score	ROC AUC	PR AUC
Negative T-axis	4.87%	94.44%	7.79%	3.24%	6.26%	38.13%	2.59%
Support Vector Machine	69.85%	72.22%	69.93%	7.47%	13.54%	74.59%	7.90%
Logistic Regression	72.10%	72.22%	72.10%	8.02%	14.44%	74.16%	9.16%
Multilayer Perceptron	70.04%	72.22%	70.11%	7.51%	13.61%	73.02%	9.00%

D. LIMITATION

With so many machine learning algorithms available, it is difficult to determine how the features are generated. Instead, we used the most commonly interpreted ECG parameters in various machine learning classifiers to develop a commercial ECG-based system that might not be the best fitted features for each machine learning algorithm. The state of the art in the field is using ECG raw voltage signals directly to generate features for deep learning [51]–[55]. Our work is limited by using a less sophisticated approach and future ECG works that incorporate deep learning would be helpful. In addition, although the performance of the proposed machine learning for MVP is fair according to the AUCs of the ROC curves of approximately 73-75%, the merit of this work is to provide an acceptable ECG tool for the early detection of a clinically important structural cardiac disease in young adults.

V. CONCLUSION

This study extends previous knowledge that using various machine learning classifiers such as the SVM, LR and MLP, through an ECG-based system with additional inputs of a few biological parameters can acceptably predict the presence of MVP compared with the traditional ECG criterion of an inverted T-wave in inferior limb leads for MVP in young male adults. Future studies should be performed to clarify the validity of the performance of the proposed machine learning methods via an ECG-based system operated specifically for young female adults.

REFERENCES

[1] L. A. Freed, D. Levy, R. A. Levine, M. G. Larson, J. C. Evans, D. L. Fuller, B. Lehman, and E. J. Benjamin, "Prevalence and clinical outcome of mitral-valve prolapse," *New England J. Med.*, vol. 341, no. 1, pp. 1–7, Jul. 1999.

[2] R. B. Devereux, E. C. Jones, M. J. Roman, B. V. Howard, R. R. Fabsitz, J. E. Liu, V. Palmieri, T. K. Welty, and E. T. Lee, "Prevalence and correlates of mitral valve prolapse in a population-based sample of American Indians: The strong heart study," *Amer. J. Med.*, vol. 111, no. 9, pp. 679–685, Dec. 2001.

[3] J. M. Flack, J. H. Kvasnicka, J. M. Gardin, S. S. Gidding, T. A. Manolio, and D. R. Jacobs, "Anthropometric and physiologic correlates of mitral valve prolapse in a biethnic cohort of young adults: The CARDIA study," *Amer. Heart J.*, vol. 138, no. 3, pp. 486–492, Sep. 1999.

[4] R. B. Devereux, I. Hawkins, R. Kramer-Fox, E. M. Lutas, I. W. Hammond, M. C. Spitzer, C. Hochreiter, R. B. Roberts, R. N. Belkin, P. Kligfield, W. TedBrown, N. Niles, M. H. Alderman, J. S. Borer, and J. H. Laragh, "Complications of mitral valve prolapse. Disproportionate occurrence in men and older patients," *Am. J. Med.*, vol. 81, no. 5, pp. 751–758, Nov. 1986.

[5] P.-Y. Liu, K.-Z. Tsai, Y.-P. Lin, C.-S. Lin, H.-C. Zeng, E. Takimoto, and G.-M. Lin, "Prevalence and characteristics of mitral valve prolapse in military young adults in Taiwan of the CHIEF heart study," *Sci. Rep.*, vol. 11, no. 1, p. 2719, Feb. 2021.

[6] D. D. Savage, R. J. Garrison, R. B. Devereux, W. P. Castelli, S. J. Anderson, D. Levy, P. M. McNamara, J. Stokes, III, W. B. Kannel, and M. Feinleib, "Mitral valve prolapse in the general population. I. epidemiologic features: The Framingham study," *Amer. Heart. J.*, vol. 106, no. 3, pp. 571–576, Sep. 1983.

[7] R. A. Levine *et al.*, "Mitral valve disease–morphology and mechanisms," *Nature Rev. Cardiol.*, vol. 12, no. 12, pp. 689–710, Dec. 2015.

[8] C. V. Leier, T. D. Call, P. K. Fulkerson, and C. F. Wooley, "The spectrum of cardiac defects in the Ehlers-Danlos syndrome, types I and III," *Ann. Int. Med.*, vol. 92, pp. 171–178, Feb. 1980.

[9] K. Hirata, F. Triposkiadis, E. Sparks, J. Bowen, H. Boudoulas, and C. F. Wooley, "The Marfan syndrome: Cardiovascular physical findings and diagnostic correlates," *Amer. Heart J.*, vol. 123, no. 3, pp. 743–752, Mar. 1992.

[10] R. B. Devereux, W. T. Brown, R. Kramer-Fox, and I. Sachs, "Inheritance of mitral valve prolapse: Effect of age and sex on gene expression," *Ann. Int. Med.*, vol. 97, no. 6, pp. 826–832, Dec. 1982.

[11] K. D. Boudoulas, A. A. Pitsis, E. L. Mazzaferri, R. J. Gumina, F. Triposkiadis, and H. Boudoulas, "Floppy mitral valve/mitral valve prolapse: A complex entity with multiple genotypes and phenotypes," *Prog. Cardiovascular Diseases*, vol. 63, no. 3, pp. 308–326, May 2020.

[12] P. A. N. Chandraratna, "On the frequency of early systolic clicks in mitral valve prolapse," *Cardiology*, vol. 62, nos. 4–6, pp. 315–321, 1977.

[13] N. Fukuda, T. Oki, K. Kawano, T. Okumoto, S. Emi, T. Uchida, T. Kawano, A. Iuchi, and H. Mori, "Systolic clicks in mitral valve prolapse: Their pathophysiological relationship to the grade and causes of prolapse," *J. Cardiol.*, vol. 18, pp. 45–52, Jan. 1988.

[14] N. Danchin, S. Briancon, P. Mathieu, J.-B. Dureux, P. Voiriot, I. Bairati, J.-P. Deschamps, and F. Cherrier, "Mitral valve prolapse as a risk factor for infective endocarditis," *Lancet*, vol. 333, no. 8641, pp. 743–745, Apr. 1989.

[15] S. W. MacMahon, J. K. Roberts, R. Kramer-Fox, D. M. Zucker, R. B. Roberts, and R. B. Devereux, "Mitral valve prolapse and infective endocarditis," *Amer. Heart. J.*, vol. 113, pp. 1291–1298, May 1987.

[16] R. A. Nishimura, M. D. McGoon, C. Shub, F. A. Miller, Jr., D. M. Ilstrup, and A. J. Tajik, "Echocardiographically documented mitral-valve prolapse—Long-term follow-up of 237 patients," *New England J. Med.*, vol. 313, no. 21, pp. 1305–1309, Nov. 1985.

[17] R. G. Singh, R. Cappucci, R. Kramer-Fox, M. J. Roman, P. Kligfield, J. S. Borer, C. Hochreiter, O. W. Isom, and R. B. Devereux, "Severe mitral regurgitation due to mitral valve prolapse: Risk factors for development, progression, and need for mitral valve surgery," *Amer. J. Cardiol.*, vol. 85, no. 2, pp. 193–198, Jan. 2000.

[18] O. C. Yontar, K. Karaagac, E. Tenekecioglu, A. Tutuncu, M. Demir, and M. Melek, "Assessment of ventricular repolarization inhomogeneity in patients with mitral valve prolapse: Value of T wave peak to end interval," *Int. J. Clin. Exp. Med.*, vol. 7, no. 8, pp. 2173–2178, Aug. 2014.

[19] Y. Turker, M. Ozaydin, G. Acar, M. Ozgul, Y. Hoscan, E. Varol, A. Dogan, D. Erdogan, and H. Yucel, "Predictors of ventricular arrhythmias in patients with mitral valve prolapse," *Int. J. Cardiovascular Imag.*, vol. 26, no. 2, pp. 139–145, Feb. 2010.

[20] I. Zegri-Reiriz, A. D. Alarcón, P. Muñoz, M. M. Sellés, V. González-Ramallo, J. M. Miro, C. Falces, C. G. Rico, X. K. Urkola, J. A. Lepe, R. R. Alvarez, J. M. R. Iglesias, E. Navas, F. Dominguez, and P. Garcia-Pavia, "Infective endocarditis in patients with bicuspid aortic valve or mitral valve prolapse," *J. Amer. College Cardiol.*, vol. 71, no. 24, pp. 2731–2740, Jun. 2018.

[21] Z. R. Bhutto, J. T. Barron, P. R. Liebson, E. F. Uretz, and J. E. Parrillo, "Electrocardiographic abnormalities in mitral valve prolapse," *Amer. J. Cardiol.*, vol. 70, no. 2, pp. 265–266, Jul. 1992.

[22] W. A. Pocock and J. B. Barlow, "Etiology and electrocardiographic features of the billowing posterior mitral leaflet syndrome: Analysis of a further 130 patients with a late systolic murmur or nonejection systolic click," *Amer. J. Med.*, vol. 51, no. 6, pp. 731–739, Dec. 1971.

[23] G.-M. Lin, M.-J. Chen, C.-H. Yeh, Y.-Y. Lin, H.-Y. Kuo, M.-H. Lin, M.-C. Chen, S. D. Lin, Y. Gao, A. Ran, and C. Y. Cheung, "Transforming retinal photographs to entropy images in deep learning to improve automated detection for diabetic retinopathy," *J. Ophthalmol.*, vol. 2018, Sep. 2018, Art. no. 2159702.

[24] S.-I. Pao, H.-Z. Lin, K.-H. Chien, M.-C. Tai, J.-T. Chen, and G.-M. Lin, "Detection of diabetic retinopathy using bichannel convolutional neural network," *J. Ophthalmol.*, vol. 2020, Jun. 2020, Art. no. 9139713.

[25] M.-J. Chen, P.-H. Yang, M.-T. Hsieh, C.-H. Yeh, C.-H. Huang, C.-M. Yang, and G.-M. Lin, "Machine learning to relate $PM_{2.5}$ and PM_{10} concentrations to outpatient visits for upper respiratory tract infections in Taiwan: A nationwide analysis," *World J. Clin. Cases*, vol. 6, no. 8, pp. 200–206, Aug. 2018.

[26] G.-M. Lin and H. H.-S. Lu, "A 12-lead ECG-based system with physiological parameters and machine learning to identify right ventricular hypertrophy in young adults," *IEEE J. Transl. Eng. Health Med.*, vol. 8, May 2020, Art. no. 1900510.

[27] G.-M. Lin and K. Liu, "An electrocardiographic system with anthropometrics via machine learning to screen left ventricular hypertrophy among young adults," *IEEE J. Transl. Eng. Health Med.*, vol. 8, Apr. 2020, Art. no. 1800111.

[28] G.-M. Lin, M. Nagamine, S.-N. Yang, Y.-M. Tai, C. Lin, and H. Sato, "Machine learning based suicide ideation prediction for military personnel," *IEEE J. Biomed. Health Informat.*, vol. 24, no. 7, pp. 1907–1916, Jul. 2020.

[29] A. E. Teijeiro, M. Shokrekhodaei, and H. Nazeran, "The conceptual design of a novel workstation for seizure prediction using machine learning with potential eHealth applications," *IEEE J. Transl. Eng. Health Med.*, vol. 7, May 2019, Art. no. 2900110.

[30] D. P. Yadav, A. Sharma, M. Singh, and A. Goyal, "Feature extraction based machine learning for human burn diagnosis from burn images," *IEEE J. Transl. Eng. Health Med.*, vol. 7, Jul. 2019, Art. no. 1800507.

[31] G. H. Tison, J. Zhang, F. N. Delling, and R. C. Deo, "Automated and interpretable patient ECG profiles for disease detection, tracking, and discovery," *Circulation, Cardiovascular Qual. Outcomes*, vol. 12, no. 9, Sep. 2019, Art. no. e005289.

[32] G. M. Lin, Y. H. Li, C. J. Lee, J. C. Shiang, K. H. Lin, K. W. Chen, Y. J. Chen, C. F. Wu, B. S. Lin, Y. S. Yu, F. Lin, F. Y. Su, and C. H. Wang, "Rationale and design of the cardiorespiratory fitness and hospitalization events in armed forces study in Eastern Taiwan," *World J. Cardiol.*, vol. 8, no. 8, pp. 464–471, Aug. 2016.

[33] Y. J. Chen, K. W. Chen, Y. L. Shih, F. Y. Su, Y. P. Lin, F. C. Meng, F. Lin, Y. S. Yu, C. L. Han, C. H. Wang, J. W. Lin, T. Y. Hsieh, Y. H. Li, and G. M. Lin, "Chronic hepatitis B, nonalcoholic steatohepatitis and physical fitness of military males: CHIEF study," *World J. Gastroenterol.*, vol. 23, no. 25, pp. 4587–4594, Jul. 2017.

[34] K.-W. Chen, F.-C. Meng, Y.-L. Shih, F.-Y. Su, Y.-P. Lin, F. Lin, J.-W. Lin, W.-K. Chang, C.-J. Lee, Y.-H. Li, C.-B. Hsieh, and G.-M. Lin, "Sex-specific association between metabolic abnormalities and elevated alanine aminotransferase levels in a military cohort: The CHIEF study," *Int. J. Environ. Res. Public Health*, vol. 15, no. 3, p. 545, Mar. 2018.

[35] K.-Z. Tsai, J.-W. Lin, F. Lin, F.-Y. Su, Y.-H. Li, Y.-P. Lin, Y.-K. Lin, C.-L. Han, C.-B. Hsieh, and G.-M. Lin, "Association of betel nut chewing with exercise performance in a military male cohort: The CHIEF study," *J. Roy. Army Med. Corps*, vol. 164, no. 6, pp. 399–404, Nov. 2018.

[36] J.-W. Lin, K.-Z. Tsai, K.-W. Chen, F.-Y. Su, Y.-H. Li, Y.-P. Lin, C.-L. Han, F. Lin, Y.-K. Lin, C.-B. Hsieh, and G.-M. Lin, "Sex-specific association between serum uric acid and elevated alanine aminotransferase in a military cohort: The CHIEF study," *Endocrine, Metabolic Immune Disorders, Drug Targets*, vol. 19, no. 3, pp. 333–340, Apr. 2019.

[37] W.-H. Chao, F.-Y. Su, F. Lin, Y.-S. Yu, and G.-M. Lin, "Association of electrocardiographic left and right ventricular hypertrophy with physical fitness of military males: The CHIEF study," *Eur. J. Sport Sci.*, vol. 19, no. 9, pp. 1214–1220, Oct. 2019.

[38] F.-Y. Su, Y.-H. Li, Y.-P. Lin, C.-J. Lee, C.-H. Wang, F.-C. Meng, Y.-S. Yu, F. Lin, H.-T. Wu, and G.-M. Lin, "A comparison of Cornell and Sokolow–Lyon electrocardiographic criteria for left ventricular hypertrophy in a military male population in Taiwan: The cardiorespiratory fitness and hospitalization events in armed forces study," *Cardiovascular Diagnosis Therapy*, vol. 7, no. 3, pp. 244–251, Jun. 2017.

[39] F.-C. Meng, Y.-P. Lin, F.-Y. Su, Y.-S. Yu, and G.-M. Lin, "Association between electrocardiographic and echocardiographic right ventricular hypertrophy in a military cohort in Taiwan: The CHIEF study," *Indian Heart J.*, vol. 69, no. 3, pp. 331–333, May/Jun. 2017.

[40] K.-Z. Tsai, S.-W. Lai, C.-J. Hsieh, C.-S. Lin, Y.-P. Lin, S.-C. Tsai, P.-S. Chung, Y.-K. Lin, T.-C. Lin, C.-L. Ho, C.-L. Han, Y. Kwon, C.-B. Hsieh, and G.-M. Lin, "Association between mild anemia and physical fitness in a military male cohort: The CHIEF study," *Sci. Rep.*, vol. 9, no. 1, p. 11165, Aug. 2019.

[41] S.-C. Lu, F.-Y. Liu, C.-J. Hsieh, F.-Y. Su, T. Y. Wong, M.-C. Tai, J.-T. Chen, and G.-M. Lin, "Quantitative physical fitness measures inversely associated with myopia severity in military males: The CHIEF study," *Amer. J. Men's Health*, vol. 13, no. 5, Sep./Oct. 2019, Art. no. 155798831988376.
[42] F.-Y. Su, S.-H. Wang, H. H.-S. Lu, and G.-M. Lin, "Association of tobacco smoking with physical fitness of military males in Taiwan: The CHIEF study," *Can. Respiratory J.*, vol. 2020, Jan. 2020, Art. no. 5968189.
[43] Y. Suresh, L. Kumar, and S. K. Rath, "Statistical and machine learning methods for software fault prediction using CK metric suite: A comparative analysis," *ISRN Softw. Eng.*, vol. 2014, Mar. 2014, Art. no. 251083.
[44] N. V. Chawla, K. W. Bowyer, L. O. Hall, and W. P. Kegelmeyer, "SMOTE: Synthetic minority oversampling technique," *J. Artif. Intell. Res.*, vol. 16, pp. 321–357, Jun. 2002.
[45] G. E. A. P. A. Batista, R. C. Prati, and M. C. Monard, "A study of the behavior of several methods for balancing machine learning training data," *ACM SIGKDD Explor. Newslett.*, vol. 6, no. 1, pp. 20–29, Jun. 2004.
[46] B. Scholkopf, *Learning With Kernels: Support Vector Machines, Regularization, Optimization, and Beyond*. Cambridge, MA, USA: MIT Press, 2001.
[47] D. W. Hosmer and S. Lemeshow, *Applied Logistic Regression*. Hoboken, NJ, USA: Wiley, 2004.
[48] J. Patterson and A. Gibson, *Deep Learning: A Practitioner's Approach*. Sebastopol, CA, USA: O'Reilly Media, 2017.
[49] F. Pedregosa, G. Varoquaux, A. Gramfort, V. Michel, B. Thirion, O. Grisel, M. Blondel, P. Prettenhofer, R. Weiss, V. Dubourg, J. Vanderplas, A. Passos, D. Cournapeau, M. Brucher, M. Perrot, and E. Duchesnay, "Scikit-learn: Machine learning in Python," *J. Mach. Learn. Res.*, vol. 12, pp. 2825–2830, Nov. 2011.
[50] K. Hajian-Tilaki, "Receiver operating characteristic (ROC) curve analysis for medical diagnostic test evaluation," *Caspian J. Int. Med.*, vol. 4, no. 2, pp. 627–635, Mar. 2013.
[51] Z. I. Attia, S. Kapa, F. Lopez-Jimenez, P. M. McKie, D. J. Ladewig, G. Satam, P. A. Pellikka, M. Enriquez-Sarano, P. A. Noseworthy, T. M. Munger, S. J. Asirvatham, C. G. Scott, R. E. Carter, and P. A. Friedman, "Screening for cardiac contractile dysfunction using an artificial intelligence–enabled electrocardiogram," *Nature Med.*, vol. 25, no. 1, pp. 70–74, Jan. 2019.
[52] Z. I. Attia, P. A. Noseworthy, F. Lopez-Jimenez, S. J. Asirvatham, A. J. Deshmukh, B. J. Gersh, R. E. Carter, X. Yao, A. A. Rabinstein, B. J. Erickson, S. Kapa, and P. A. Friedman, "An artificial intelligence-enabled ECG algorithm for the identification of patients with atrial fibrillation during sinus rhythm: A retrospective analysis of outcome prediction," *Lancet*, vol. 394, no. 10201, pp. 861–867, Sep. 2019.
[53] F. Lopez-Jimenez, Z. Attia, A. M. Arruda-Olson, R. Carter, P. Chareonthaitawee, H. Jouni, S. Kapa, A. Lerman, C. Luong, J. R. Medina-Inojosa, P. A. Noseworthy, P. A. Pellikka, M. M. Redfield, V. L. Roger, G. S. Sandhu, C. Senecal, and P. A. Friedman, "Artificial intelligence in cardiology: Present and future," *Mayo Clin. Proc.*, vol. 95, no. 5, pp. 1015–1039, May 2020.
[54] A. K. Feeny, M. K. Chung, A. Madabhushi, Z. I. Attia, M. Cikes, M. Firouznia, P. A. Friedman, M. M. Kalscheur, S. Kapa, S. M. Narayan, P. A. Noseworthy, R. S. Passman, M. V. Perez, N. S. Peters, J. P. Piccini, K. G. Tarakji, S. A. Thomas, N. A. Trayanova, M. P. Turakhia, and P. J. Wang, "Artificial intelligence and machine learning in arrhythmias and cardiac electrophysiology," *Circulation, Arrhythmia Electrophysiol.*, vol. 13, no. 8, Aug. 2020, Art. no. e007952.
[55] W.-Y. Ko, K. C. Siontis, Z. I. Attia, R. E. Carter, S. Kapa, S. R. Ommen, S. J. Demuth, M. J. Ackerman, B. J. Gersh, A. M. Arruda-Olson, J. B. Geske, S. J. Asirvatham, F. Lopez-Jimenez, R. A. Nishimura, P. A. Friedman, and P. A. Noseworthy, "Detection of hypertrophic cardiomyopathy using a convolutional neural network-enabled electrocardiogram," *J. Amer. College Cardiol.*, vol. 75, no. 7, pp. 722–733, Feb. 2020.

GEN-MIN LIN (Member, IEEE) received the M.D. degree from the National Defense Medical Center, Taiwan, in 2003, the M.P.H. degree from Tzu Chi University, Taiwan, in 2012, and the Ph.D. degree in electrical engineering from National Dong Hwa University, Taiwan, in 2018. He was a Resident and a Cardiology Fellow with Tri-Service General Hospital, Taiwan. He joined Hualien Armed Forces General Hospital, Taiwan, in 2009. He became the Chief of the Department of Internal Medicine, Hualien Armed Forces General Hospital, in 2019, and was promoted to a Colonel in Air Forces, Taiwan. From 2019 to 2020, he was an Adjunct Assistant Professor with the Department of Preventive Medicine, Northwestern University, USA. His research interests include cardiovascular medicine, epidemiology study, signal analysis, and artificial intelligence in medicine. He became a fellow of the American Heart Association (AHA), in 2020.

HUAN-CHANG ZENG finished his Ph.D. thesis on genetic regulation of differentiation of mesenchymal stem cells with the Dr. Brendan Lee's Laboratory, Baylor College of Medicine, and identified the critical role of the microRNA miR-23a cluster on regulating TGF-β signaling during differentiation of osteoblastic lineages (Nature Communications, PMID: 28397831). He also found microRNA miR-34c can affect osteoblast and osteoclast differentiation by targeting the Notch receptors (Molecular Human Genetics, PMID: 22498974). In addition, gain of function of Notch was proved as a key driver of osteosarcoma development (Cancer Cell, PMID: 25203324). He was involved in the projects of undiagnosed diseases network (UDN) using CRISPR-Cas9 genomic editing, to generate cell/animal models. He is currently the Founder and the CEO of GENEus Medical Technology Company to provide clinical-grade cutting-edge genetic services.